Iranian Journal of Hydrogen & Fuel Cell 2(2015) 99-107

Iranian Journal of Hydrogen & Fuel Cell

IJHFC

Journal homepage://ijhfc.irost.ir

Electrochemical Study of the Hydrogen Adsorption/Reduction (HAR) Reaction on Graphene Oxide as an Electrocatalyst for Proton Exchange Membrane Fuel Cells

Alireza Rahmanian [1], Leila Naji[1,*], Mehran Javanbakht[1,2]

[1] Department of Chemistry, AmirKabir University of Technology, 424 Hafez Avenue, Tehran P.O Box: 15875-4413, Iran.
[2] Renewable Energy Research Center, AmirKabir University of Technology (Polytechnic), 424 Hafez Avenue, Tehran, P.O Box: 15875-4413, Iran. Tehran

Article Information

Article History:

Received:
15 November 2015
Received in revised form:
11 December 2015
Accepted:
13 December 2015

Keywords

Graphene oxide
HAR reaction
Proton exchange membrane fuel cell

Abstract

In the current work, graphene oxide (GO) samples were prepared at room temperature from graphite flakes using a modified Hummer's method to produce metal-free electrocatalysts. The effect of the duration of the oxidation process on the structural, chemical and physical characteristics of the GO samples was evaluated using X-ray diffraction (XRD), Fourier transform infrared spectroscopy (FTIR), ion-exchange capacity (IEC) measurements and Field-emission scanning electron microscopy (FESEM). Electrochemical behavior of the GO samples towards hydrogen adsorption/reduction (HAR) reactions was evaluated using a typical three-electrode electrochemical cell at room temperature under N_2 atmosphere. Increasing the oxidation time from 3 h to 5 h resulted in dramatic decreases in the number of epoxy and carboxyl groups, interlayer spacing (~ 9.5%) and also in the IEC (~ 1.8 times) of the GO samples. Moreover, increasing the oxidation time resulted in a remarkable increase in the size of the GO sheets along two dimensions (~ 1.5 times) and also in the electrochemical surface area (ECSA) of GO (~60%). CV studies revealed that increasing the oxidation time results in an increase in the current response of GO samples towards the HAR reaction, indicating an enhancement in the electrochemical activity of GO. This was attributed to the formation of larger GO samples with an improved electronic network.

1. Introduction

Proton exchange membrane fuel cells (PEMFCs) are widely recognized as one of the most promising technologies for power generation due to their high efficiency, high power density, rapid start-up/shut-down, low weight, compactness and suitability for discontinuous operation [1]. Platinum and platinum alloys are commonly used as catalyst in the fabrication of low temperature fuel cells. They are supported on a high surface area substrate to obtain a high dispersion and narrow distribution of catalyst

*Corresponding Author's E-mail address: leilanaji@aut.ac.ir (L. Naji)
Tel: +98 (21) 64542767; Fax: +98 (21) 64542762;

nanoparticles which is the prerequisite to obtain high catalytic performance [2, 3]. The catalyst support materials can also modify the electronic properties of the catalyst nanoparticles which in turn affects the reaction characteyristics of the active sites at its surface. The type of catalyst support material greatly influences the cost, performance, stability and durability of PEMFCs. The support materials are required to possess high specific surface area, high conductivity, thermal and electrochemical stability under fuel cell operating conditions and also have a strong interaction with catalytic metals [3]. Carbon materials have been considered as ideal catalyst support in PEMFCs due to their large specific surface area, high electrical conductivity, and pore structures. Graphene (Gr) as a newly discovered allotrope of carbon possesses a unique two dimensional structure composed of sp^2- bonded carbon atoms which are only one atom thick [4]. Gr can be used as the catalyst and also the catalyst support because of its superior electrical conductivities compared to graphitic carbon, and its unique outstanding physical and chemical properties [6, 5]. However, the inert and hydrophobic nature of Gr will be the rate limiting steps in considering Gr as a metal catalyst support [6, 5]. Graphene oxide (GO) possesses oxygen containing functional groups, such as hydroxyl, epoxide, and carboxyl groups, and can be applied as the catalyst support [1]. The presence of such functional groups makes GO a good support for uniform dispersing and depositing of platinum nanoparticles. However, in comparison to Gr, GO has a drastically lower conductivity and stability as a result of the conjugated sp^2 network loss [1, 7]. The presence of oxygen-containing functional groups on GO leads to the formation of a single (or a few) layer(s) of Gr nanosheets which are more accessible for the embedment of metal catalysts. Such functionalized Gr nanosheets have a better adhesion to the catalytic nanoparticles [1, 8, 9]. Introducing proton-conducting carboxyl groups on the Gr sheets enhances the effective triple-phase boundary (TPB) and the stability of catalysts which are essential for prolonged performance of PEMFCs [2, 7, 8]. It has been established that using GO as the catalyst support can enhance catalytic activities towards the oxygen reduction reaction (ORR) and facilitate the transfer of reaction species [8-11]. GO features unique advantages for designing catalysis due to a tunable molecular structure, abundance and strong tolerance to acid/alkaline environments. Recent advances in low-dimensional carbon materials as metal-free catalysts have shown their promising future in energy related electrocatalytic oxygen reduction and evolution reactions [12]. However, this innovative concept has not yet been explored for the hydrogen adsorption/reduction (HAR) reaction. In this study GO samples were prepared from graphite flakes at room temperature using a modified Hummer's method. The electrochemical behavior of GO towards the (HAR) reaction was investigated using the cyclic voltammetry (CV) technique. The oxidation time of graphite sheets was varied to study the effect of this parameter on the structural, physicochemical and electrochemical behavior of GO samples towards HAR reactions. GO samples were studied using Fourier transform infrared (FTIR) spectroscopy. Interlayer spacing and also the dimensional ratio of GO samples were investigated by the X-ray diffraction (XRD) technique. Ion exchange capacity (IEC) of the samples was compared using the acid-base titration method. Field emission scanning electron microscopy (FESEM) was used to study the morphology of GO samples. The electrochemical behavior of GO samples towards HAR reactions were studied using atypical a three-electrode electrochemical cell at room temperature under N_2 atmosphere. Increasing the oxidation time from 3 h to 5 h resulted in dramatic decreases in the number of epoxy and carboxyl groups, interlayer spacing (~ 9.5%) and also in the IEC (~ 1.8 times) of the GO samples. Moreover, increasing the oxidation time resulted in a remarkable increase in the size of the GO sheets along two dimensions (~ 1.5 times) and also in the electrochemical surface area (ECSA) of the GO (~60%). CV studies revealed that increasing the oxidation time results in an increase in the current response of GO samples towards HAR reaction, indicating an enhancement in the electrochemical activity of the GO. This was attributed to the formation

of larger GO samples with an improved electronic network.

2. Experimental

Graphite powder (GR0012, Scharlau), concentrated sulfuric acid (H_2SO_4, 95-98%, Merck), sodium nitrate ($NaNO_3$, 99%, Merck), potassium permanganate ($KMnO_4$, 99%, Scharlau), hydrogen peroxide (H_2O_2, 31%, Dr. Mojallali Chemical Labs), sodium chloride (NaCl, Merck), sodium hydroxide (NaOH, ACS reagent, +97.0%, Sigma-Aldrich), sodium borohydride ($NaBH_4$, 98%, Scharlau) and Nafion solution (5%, DuPont) were used as supplied without further purification and modification.

2.1. Synthesis of GO

According to modified Hummers methods [13] 1 g of graphite powder and 1 g of $NaNO_3$ were added to 150 ml H_2SO_4 (98%) in a flask and stirred for an hour in an ice water bath. Then, 3 g of $KMnO_4$ (99%) were added gradually over 2 h to the flask and the mixture was stirred at 40°C for 3 h. Half of the mixture was then transferred to another flask and mixed with 15 ml deionized water over 30 min, while stirring, and then diluted with 20 ml of DI water. In order to eliminate oxidant ions, 1 ml of H_2O_2 (31%) was added to the flask and the mixture was centrifuged for 30 min at 6000 rpm. The brown residues (Figure 1 part (a)), was rinsed and centrifuged eight times with deionized water. The resulted purified GO was then dried in an oven at 50°C for 1 h and stored as powder. This sample was called GO_3 to indicate the oxidation duration of 3 h. The rest of the mixture was stirred and heated at 40 °C for another 2 h and the color of the mixture turned purplish brown (Figure 1 part (b)). Deionized water and H_2O_2 were then added to the mixture through a similar procedure described for the preparation of GO_3 samples. This sample was then called GO_5 to show the oxidation duration of 5 h.

Reduced graphene oxide (rGO) was synthesized by reducing GO using $NaBH_4$. To this end, 30 mg of GO_5 sample was dispersed in 50 ml deionized water then 75 ml 0.5 M $NaBH_4$ solution was added dropwise to the GO dispersion over 2 h while stirring at 70°C. Then, the black residues (rGO), was rinsed and centrifuged with deionized water repeatedly. The resulted purified GO was then dried in an oven at 50°C for 1 h and stored as powder.

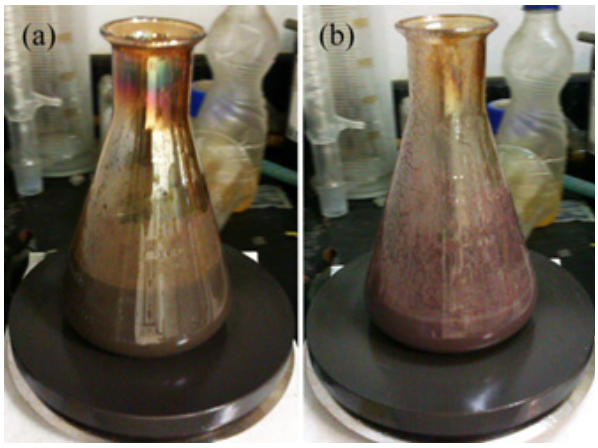

Fig. 1.Digital images of (a) GO_3 and (b) GO_5 mixtures during oxidation process.

2.2. Physicochemical characterization of GO

FTIR spectra were acquired from an Alpha Bruker spectrometer as transmittance data. KBr was used as reference material to prepare a sample pellet.

IEC measurements were performed using the acid-base titration method [1]. To exchange all acidic protons on GO samples with Na^+ ions 0.01 g of GO was dispersed in 1 ml saturated NaCl aqueous solution and left for 24 h at room temperature. The mixture was then centrifuged for 30 min at 6000 rpm and GO was separated. The clear solution was titrated by a 0.01 M NaOH solution using phenolphthalein as an indicator. The equivalent weight (EW) was calculated according to Equation 1[1]:

$$EW = \frac{W}{V_{NaOH} \times C_{NaOH}} \quad (1)$$

Where C_{NaOH} and V_{NaOH} are the concentration and volume of NaOH solution required for neutralization of the residual solution, respectively, and W is the weight of the GO samples.

XRD patterns were obtained using EQUINOX3000 Intel with a Cu/Kα source, operated at 40 KV and 30 mA with a scanning rate of 10º min^{-1} (2º<2θ<120º). The Bragg's law equation (Equation 2) was used to calculate interlayer spacing between GO layers and Scherrer's equation (Equation 3) was applied to estimate the average width and height of the GO layers.

$$n\lambda = 2d\sin\theta \quad (2)$$

$$L = \frac{K\lambda}{\beta\cos\theta} \quad (3)$$

In Eq. 3, λ is the wavelength of source beam used, d is the interlayer spacing, θ is the scattering angle, L is the average crystallite size, K is the shape factor constant, and the β is the full width at half maximum (FWHM) of the diffraction peak, in radians [14,15].

FESEM images were taken using a Zeiss Sigma instrument. Before imaging the GO samples were dispersed in ethanol, then coated on a pre-cleaned glass slide and sputtered with a 10 nm Au layer.

2.3. Electrochemical measurement

Electrochemical measurements were performed at ambient temperature using a Metrohm Autolab electrochemical analyzer (PGSTAT302N) with a conventional three-electrode cell (A platinum rod as the counter electrode and an Ag/AgCl electrode as the reference electrode). The working electrode was prepared by pouring a suspension of catalyst onto the surface of a pre-cleaned glassy carbon electrode (GCE, d=2 mm). The catalyst suspension was prepared by mixing 2.0 mg of GO and 1 ml of ethanol and the mixture was sonicated for 15 min. Using a micropipette 4µL of the catalyst suspension was poured onto the GCE and left to dry at room temperature, and then the deposited GCE was put in an oven at 50°C for 20 min. CV response of the GO and rGO samples towards the HAR reaction was evaluated in 1 M H_2SO_4 solution at a voltage range of -1.0 and +1.0 V with a scan rate of 30 mV s^{-1}. Experiments were carried out using a three electrode setup including an Ag/AgCl reference electrode, a glassy carbon working electrode (GCE) and a platinum electrode as the auxiliary electrode. For these measurements, an aqueous suspension of GO and rGO samples with the same concentration of 4 mg/ml was prepared. Then, a same aliquot of these solutions were coated separately on the pre-cleaned GCE and left to dry at room temperature. Nitrogen (N_2) was purged through the H_2SO_4 solution for 30 min before each measurement.

3. Results and discussion

3.1. Physicochemical characterization

FTIR spectra of the synthesized GO_3, GO_5 and pristine graphite are compared in Figure 2. As can be seen, the GO samples showed much more peaks compared to graphite samples. The broad band at 3422 cm^{-1} corresponds to O-H stretching of hydroxyl and carboxyl functional groups and the strong band at

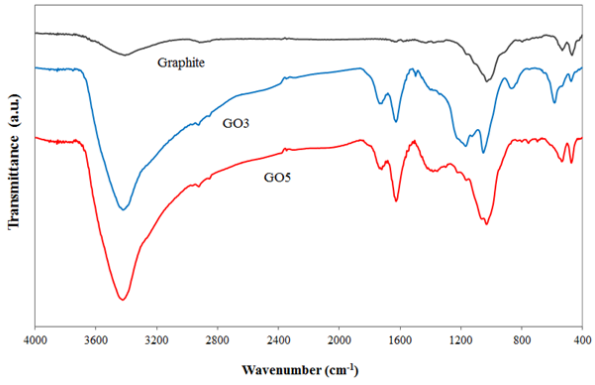

Fig. 2. FTIR spectra of pristine graphite, GO_3, and GO_5.

1734 cm^{-1} is a result of C=O stretching in carboxyl and carbonyl functional groups. In the FTIR spectrum of the GO_3 sample the band at 1628 cm^{-1} was due to C=C stretching of the Gr skeleton, a broad band at 1385 cm^{-1} was due to C-O-H bending in the hydroxyl group, a band at 1224 cm^{-1} was a result of C-OH stretching of the carboxyl groups, a band at 1169 was due to asymmetric stretching of C-O in the epoxy groups, a strong band at 1052 was due to C-OH stretching of hydroxyl groups and a medium and broad band

at 869 was a result of symmetric C-O stretching of epoxy and out of plane bending of O-H in the carboxyl groups [16, 17]. The effect of the presence of these oxygen-containing functional groups was observed as facilitating the hydration of GO sheets in aqueous media [13]. Similar peaks were also observed for GO_5 samples. However, the intensity of some peaks were intensified for the GO_5 sample while others were attenuated. As Figure 2 shows, for the GO_5 sample the intensity of the bands related to the epoxy and carboxyl functional groups decreased while the intensity of the bands related to the hydroxyl groups increased compared to that of the GO_3 sample. This indicates that increasing the duration of the oxidation process results in a significant change in the number and the type of oxygen-containing functional groups on GO nanosheets. This was confirmed by the results obtained from IEC measurements of the GO samples. IEC measurements were carried out to determine the carboxylic acid content of the GO_3 and GO_5 samples. The results revealed that the EW of the GO_3 and GO_5 samples were about 155 and 278g eq^{-1}, respectively, indicating the presence of a higher percentage (79%) of the carboxylic acid groups on the GO_3 sample.

Figure 3 compares the XRD patterns of pristine graphite, GO_3 and GO_5 samples. The Bragg's equation was applied to the (002) reflection to evaluate the interlayer spacing of the samples denoted as d [13, 18]. A strong peak of pristine graphite appears at $2\theta = 26.6°$ which corresponds to a Bragg spacing of about 0.335 nm. The XRD pattern of GO_3 exhibits a strong peak at $2\theta = 10.5°$ which correspond to an interlayer spacing of about 0.840 nm. The observed difference in the interlayer spacing of graphite and the GO_3 sample is attributed to the presence of oxygen-containing functional groups on the GO nanosheets. For the GO_5 sample a strong peak appeared at

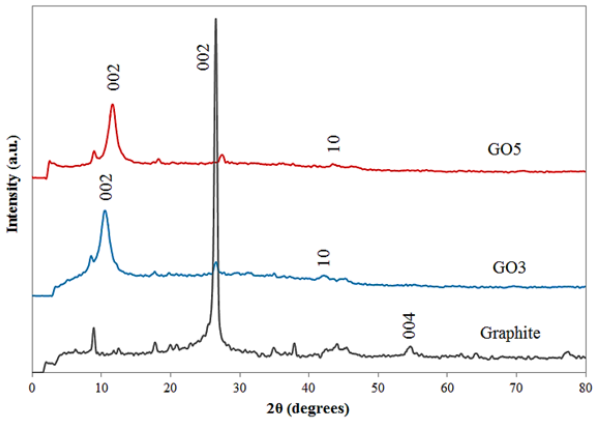

Fig. 3. XRD patterns of pristine graphite, GO_3, and GO_5.

$2\theta = 11.6°$ which corresponds to an interlayer spacing of about 0.763 nm. As the results imply, increasing the duration of the oxidation process from 3 h to 5 h led to a decrease in the interlayer spacing of the GO nanosheets in the GO_5 sample compared to that of the GO_3 sample. This shows that the number of oxygenated functional groups has decreased in the case of the GO_5 sample. This is in good agreement with the FTIR (Figure 2) and IEC data of the GO samples discussed previously. The Scherer equation with a shape factor of 0.9 was applied to the (002) reflection to evaluate the average height of stacking layers of the GO samples, denoted as H. The Scherer equation was also applied with a Warren constant of 1.84 to the two-dimensional (10) reflection for determining the average width of stacking layers of the GO samples, denoted as D [18]. The XRD data was summarized in Table 1. The XRD pattern of graphite did not show any two-dimensional reflection and therefore the average height of graphite flakes was not calculated. Results indicated that the stacking layers of GO_3 had dimensions of 13.9 nm × 5.7 nm (average width by height) equal to about 6-7 layers and GO_5 had dimensions of 20.8 nm × 6.2 nm

Table 1. Summarized XRD data of graphite and GO samples.

Sample	Reflection (002)					Reflection (10)		
	2θ (deg)	FWHM (deg)	d (nm)	H (nm)	n	2θ (deg)	FWHM (deg)	D (nm)
Graphite	26.6	0.51	0.335	16.0	47-48	-	-	-
GO_3	10.5	1.40	0.840	5.7	6-7	42.1	1.25	13.9
GO_5	11.6	1.28	0.763	6.2	8-9	43.6	0.84	20.8

(average width by height) with about 8-9 layers in each stack. Schematic illustration of the GO_3 and GO_5 stacking layers are shown in Figure 4. Graphite flakes contain about 47-48 layers in each stack. XRD results demonstrate that the exfoliation of graphite occurs through the oxidation process in which the number of layers in the GO samples decreases remarkably. Moreover, the application of a longer oxidation time resulted in a decrease in the number of oxygenated functional groups (see Figure 2) and an increase in the surface dimension of the GO stacking layers. Graphene oxide is a two-dimensional nanoparticle featuring a variety of chemically reactive functional groups, such as epoxy and hydroxyl groups, on the basal plane and carboxylic acid groups along the sheet edge. Regardless of these surface moieties, a significant

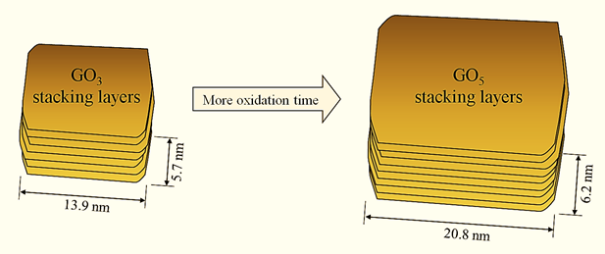

Fig. 4. Schematic representation of dimensional ratio of GO_3 and GO_5 samples.

amount of the sp^2 – hybridized carbon backbone structure remains intact during the oxidation, allowing the GO samples to retain a high degree of planarity and a correspondingly high surface-to-volume ratio [16, 19]. FTIR and XRD results revealed that the GO_5 sample possesses a lower number of carboxyl groups and also a larger surface dimension (~1.5 times). Thus, it can be concluded that after 3 h no significant oxidation occurs. Results also imply that over longer oxidation time GO sheets are brought together side-by-side and form larger GO sheets. The residual sp^2 – hybridized carbon domains in GO can contribute to the attraction between GO sheets. These forces can also lead to layer-by-layer deposition of GO sheets. As discussed previously, the GO_5 sample was shown to have a larger surface area and a larger number of layers in each stack. When the GO sheets are brought together side-by-side microscopic morphologies such as wrinkles, folds, and overlaps can occur through the interactions between the neighboring GO sheets. The morphology of the GO samples was studied by FESEM. Figure 5 compares the FESEM images of GO_3 (parts (a-d) and GO_5 (parts (e-h) samples. Both samples consisted of randomly aggregated, thin, crumpled sheets closely associated with each other. It is possible to distinguish the edges of the sheets, including kinked and wrinkled areas. Comparing the FESEM images of both samples in each row reveals that the GO_5 sample has a relatively larger surface area and thicker edges compared to that of the GO_3 sample. Moreover, the GO sheets are overlapped rather than aggregated.

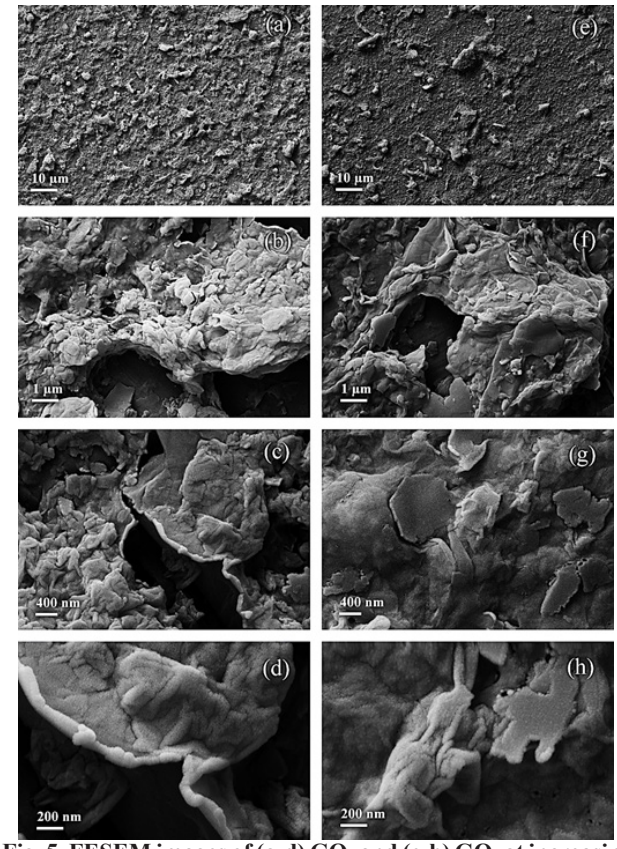

Fig. 5. FESEM images of (a-d) GO_3 and (e-h) GO_5 at increasing magnification.

3.2. Electrochemical measurements

Figure 6 parts (a) and (b) show the CV responses of the GO_3 and GO_5 samples towards the HAR reaction. The two voltammograms appeared similar in shape but different in current intensity. During anodic and cathodic sweeping of voltage three and two peaks were observed, respectively. The peaks appeared in the potential range of 0.0 and 0.35 V corresponding to the HAR reaction [6, 21]. The potential and current density of five peaks for both samples are summarized in Table 2. In order to distinguish between peaks 1 and 2 the defined region in Figure 6 (a) was shown in Figure 6 (b). As can be seen, the GO_5 sample showed a higher HAR current density compared to the GO_3 samples. This indicates that the GO_5 sample with a larger lateral dimension is more desirable for the HAR reaction and shows higher activity towards this reaction. The electrochemical surface area (ECSA) can be estimated by integrating the charge passed during the hydrogen adsorption/reduction from the GCE surface after double-layer correction. The calculated value of the ECSA of the GO_5 sample (1.61 m^2g^{-1}) was about 60% higher than that measured for the GO_3 sample. It is expected that the GO_5 sample with the larger lateral dimension possesses a more suitable electronic network for promoting the HAR process. The higher electrocatalytic activity of the GO_5 sample can be attributed to a reduction in the inter-sheet contact resistance in this sample compared to the GO_3 sample [22]. These results reveal that the electrocatalytic characteristics of GO originate from its intrinsic chemical and electronic properties which synergistically promote the proton adsorption and reduction kinetics. However, the exact mechanisms of the HAR reaction on the GO sheets is unclear and requires further experiments. A critically important structural feature of GO is the pendent acidic functional groups which are thought to facilitate hydrogen mobility.

Figure 7 compares the CV response of the GO_5 and rGO_5 samples .Only two peaks at 0.425 V in the anodic scan and 0.341 V in the cathodic scan were observed for the rGO_5 sample. These peaks appeared at the same potential as peaks 3 and 4 for the GO_5 sample. However, peaks 1, 2, and 5 were not observed

Table 2. Peak information of GO samples extracted from their voltammograms.

Sample	Axis	Anodic scan		Cathodic scan		
		Peak 1	Peak 2	Peak 3	Peak 4	Peak 5
GO3	E (V)	0.216	0.271	0.468	0.354	-0.075
	J (mA cm^{-1})	0.0376	0.0378	0.0385	0.0117	-0.0005
GO5	E (V)	0.210	0.290	0.462	0.338	-0.085
	J (mA cm^{-1})	0.0420	0.0402	0.0398	0.0144	-0.0041

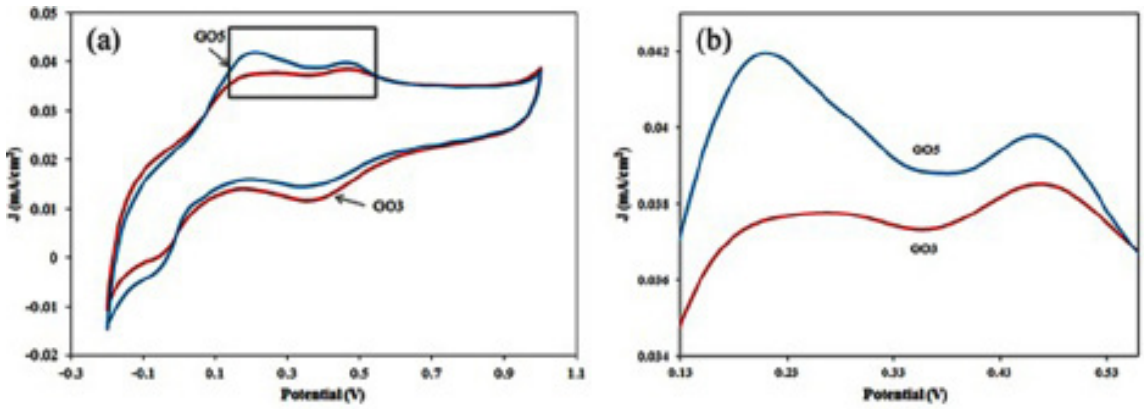

Fig. 6. (a) CV response of GO_3 and GO_5 toward HAR reaction (a) in full view and (b) in the selected region shown in part (a)

in the case of the rGO_5 sample. This was attributed to the removal of oxygenated functional groups during chemical reduction. This shows that the functional groups on the GO sheets can attend in the HAR reaction. However, the electrocatalytic activity of the rGO_5 sample towards the HAR reaction is much higher than that observed for the GO_5 sample. This implies that the removal of oxygenated functional groups via chemical reduction has a significant improving impact on the electronic network of the rGO_5 sample and improves its electrical conductivity. In other words, it facilitates the electron transfer kinetic and results in a higher current response. We believe that the electrocatalytic activity of the GO samples can be improved by altering the synthesis parameters and also by alloying GO with non-precious metals.

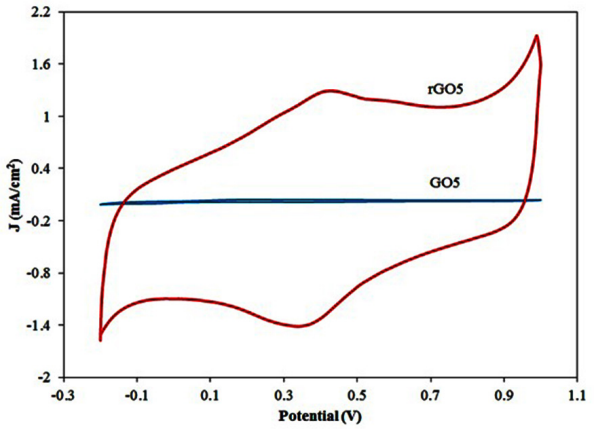

Fig. 7. Comparison of CV response of GO_5 and rGO_5 samples.

4. Conclusions

GO samples were prepared using a modified Hummer's method and the effect of the duration of the oxidation process on the structural, chemical and physical properties of GO samples was evaluated using XRD, FTIR, IEC measurements and FESEM.

Electrochemical behavior of the GO samples towards hydrogen adsorption/reduction (HAR) reactions was evaluated using a typical three-electrode electrochemical cell at room temperature under N_2 atmosphere. Increasing the oxidation time from 3 h to 5 h resulted in dramatic decreases in the number of epoxy and carboxyl groups, interlayer spacing (~ 9.5%) and also in the IEC (~ 1.8 times) of the GO samples. Moreover, increasing the oxidation time resulted in a remarkable increase in the size of the GO sheets along two dimensions (~ 1.5 times) and also in the electrochemical surface area (ECSA) of GO (~60%). CV studies revealed that increasing the oxidation time results in an increase in the current response of GO samples towards the HAR reaction, indicating an enhancement in the electrochemical activity of GO. This was attributed to the formation of larger GO samples with an improved electronic network. Experimental observations revealed that GO possesses electrocatalytic properties which originate from its intrinsic chemical and electronic properties that promotes the proton adsorption and reduction kinetics. This finding may shed light towards replacing precious and high cost noble metal with a metal-free low cost carbon-based material.

5. References:

[1] He D., Kou Z., Xiong Y., Cheng K., Chen X., Pan M., Mu S., "Simultaneous sulfonation and reduction of graphene oxide as highly efficient supports for metal nanocatalysts", Carbon, 2014, 66:312.

[2] Woo S., Lee J., Park S.K., Kim H., Chung T.D., Piao Y., "Enhanced electrocatalysis of PtRu onto graphene separated by Vulcan carbon spacer", J. Power Sources, 2013,222:261.

[3] Hsieh C.T., Liu Y.Y., Roy A.K., "Pulse electrodeposited Pdnanoclusters on graphene-based electrodes for proton exchange membrane fuel cells", Electrochimica Acta, 2012, 64:205.

[4] Zhang X., Sui Z., Xu B., Yue S., Luo Y., Zhan W.,"Mechanically strong and highly conductive graphene aerogel and its use as electrodes for electrochemical power sources", J. Mater. Chem., 2011, 21:6494.

[5] Fang Z., Liu Z., Wang Y., Ajayan P.M., Nordlander P.,

Halas N.J.,"Graphene-antenna sandwich photodetector", Nano Lett., 2012,12:3808.

[6] Wolf E. L., Applications of Graphene - An Overview, Springer, 2014.

[7] Boukhvalov D.W., Dreyer D.R., Bielawski C.W., Son Y.W., "A Computational Investigation of the Catalytic Properties of Graphene Oxide: Exploring Mechanisms by using DFT Methods", ChemCatChem, 2012, 4:1844.

[8] Jung J.H., Park H.J., Kim J., Hur S.H., "Highly durable Pt/graphene oxide and Pt/C hybrid catalyst for polymer electrolyte membrane fuel cell", J. Power Sources, 2014,248:1156.

[9] Tiido K., Alexeyeva N., Couillard M., Bock C., MacDougall B., Tammeveski K., "Graphene-TiO_2 Composite Supported Pt Electrocatalyst for Oxygen Reduction Reaction", J. Electrochimica Acta, 2013,107:509.

[10] Su C., Acik M., Takai K., Lu J., Hao S.J., Zheng Y., Wu P., Bao Q., Enoki T., Chabal Y.J., Loh K.P., "Probing the catalytic activity of porous graphene oxide and the origin of this behaviour", Nat. Commun., 2012,3:1298.

[11] Yuan L., Jiang L., Liu J., Xia Z., Wang S., Sun G., "Facile synthesis of silver nanoparticles supported on three dimensional graphene oxide/carbon black composite and its application for oxygen reduction reaction", Electrochimica Acta, 2014,135:168.

[12] Zheng Y., Jiao1 Y., Zhu Y., Li L.H., Han Y., Chen Y.,Du A., Jaroniec M., Qiao S.Z., "Hydrogen evolution by a metal-free electrocatalyst", Nat.Commun., 2014,5:3783.

[13] Moaven Sh., Naji L., Afshar Taromi F., Sharif F., "Photovoltaic Performance of Flexible Graphene/Ag Nanocomposite Electrode-Based Polymer Solar Cells under Bending", RSC Advances, 2015,5:30889.

[14] Hammond C., The Basics of Crystallography and Diffraction, Oxford University Press, 2015.

[15] Warren B. E., X-ray Diffraction, Courier Corporation, 1969.

[16] Zeng C., Tang Z., Guo B., Zhang L.,"Supramolecular ionic liquid based on graphene oxide", Phys. Chem. Chem. Phys., 2012,28:9838.

[17] Shen J., Yan B., Shi M., Ma H., Lia N., Ye M.,"One step hydrothermal synthesis of TiO2-reduced graphene oxide sheets", J. Mater. Chem., 2011, 10:3415.

[18] Stobinski L., Lesiak B., Malolepszy A., Mazurkiewicz M., Mierzwa B., Zemek J., Jiricek P., Bieloshapka I.,"Graphene oxide and reduced graphene oxide studied by the XRD, TEM and electron spectroscopy methods", J. Electron Spectrosc., 2014,195:145.

[19] Lerf A., He H., Forster M., Klinowski J., "Structure of Graphite Oxide Revisited", J. Phys. Chem. B,1998,102, 4477.

[20] Gao W., Graphene Oxide: Reduction Recipes, Spectroscopy, and Applications, Springer, 2015.

[21] Liang H.W., Cao X., Zhou F., Cui C.H., Zhang W.J., Yu S.H.,"A free-standing Pt-nanowire membrane as a highly stable electrocatalyst for the oxygen reduction reaction", Adv. Mater., 2011,23:1467.

[22] Matsumoto Y., Tateishi H., Koinuma M., Kamei Y., Ogata C., Gezuhara K., Hatakeyama K., Hayami S., Taniguchi T., Funatsu A.,"Electrolytic graphene oxide and its electrochemical properties", J. Electroanal. Chem., 2013,704:233.